Available online at www.sciencedirect.com
SCIENCE DIRECT®
Catalysis Today 105 (2005) 223–233
CATALYSIS TODAY
www.elsevier.com/locate/cattod

Mathematical modeling of rate oscillations in N_2O reduction by H_2 and CO over the Ir(1 1 0) surface

N.V. Peskov [a,*], M.M. Slinko [b,**], Sónia A.C. Carabineiro [c], Bernard E. Nieuwenhuys [c]

[a] *Moscow State University, Department of Computational Mathematics & Cybernetics, 119899 Moscow, Russia*
[b] *Institute of Chemical Physics RAS, Kosygina Str. 4, Moscow 119334, Russia*
[c] *Leiden University, Leiden Institute of Chemistry, Surface Science and Catalysis, Einsteinweg 55, 2333 CC, Leiden, The Netherlands*

Available online 27 June 2005

Abstract

Two realistic mathematical models were developed which can reproduce almost quantitatively the region of existence and the properties of the experimentally observed oscillatory behaviour for the $N_2O + H_2$ and $N_2O + CO$ reactions over the Ir(1 1 0) single crystal surface. The peculiarity of the oscillatory behaviour in these systems is the phase shift between the oscillations of the partial pressures of the two reaction products. While the oscillation maximum for H_2O is ''delayed'' compared to the maximum of N_2 oscillation, nearly anti-phase oscillations of the N_2 and CO_2 production rates were observed. Moreover, not only the products N_2 and CO_2 oscillate in counter-phase, but also the reactants N_2O and CO produce counter-phase oscillations. It was demonstrated that in both systems oscillatory behaviour could originate due to the lateral interactions in the adsorbed layer. The main feedback mechanism generating oscillations operates via the acceleration of N_2O decomposition by oxygen. The result of mathematical modeling shows that the larger phase shift of oscillations of CO_2 and N_2 production rates in comparison with the H_2O and N_2 production rates originates due to the more complicated character of lateral interactions in the adsorbed layer.

Keywords: N_2O reduction; Ir(1 1 0) surface; Mathematical modeling; Kinetic oscillations; Lateral interactions

1. Introduction

Oscillatory behaviour is frequently observed in heterogeneous catalytic systems [1]. CO and H_2 oxidation over Pt and Ni were the first systems where self-sustained oscillations of the production rate of the reaction product (CO_2 or H_2O) have been detected [2,3]. Later oscillatory behaviour was discovered in other reactions, where more than one product is produced. An example of such oscillatory system is the $NO + H_2$ reaction over Pt, Rh and Ir single crystal surfaces, where three N-containing products: N_2, NH_3 and N_2O can be formed. It was demonstrated that both the activity and the selectivity are strongly dependent on the nature and structure of the single crystal surface [4]. Two of the three possible products, namely N_2 and NH_3 oscillate with different phase shifts for various single crystal surfaces. Whereas for Pt(1 0 0), Ir(1 0 0) and Ir(5 1 0) the formation rates of N_2 and NH_3 oscillate in phase, there is a phase shift between the rates of production of N_2 and NH_3 on the Rh(1 1 1) and Rh(5 3 3) surfaces. Finally, on Ir(1 1 0) the rates of N_2 and NH_3 displayed oscillations exactly in counter-phase [4].

The analysis of the phase shifts between the products provides additional information on the reaction mechanism and helps in the development of possible mathematical models. Mathematical modeling revealed that in the case of Pt(1 0 0) an autocatalytic increase in the number of vacant sites needed for NO dissociation on Pt(1 0 0)-(1 × 1) [5] or the (1 × 1) ⇔ hex surface phase transition of Pt(1 0 0) [6,7] are the essential steps in the oscillation mechanism and are responsible for the in-phase oscillations of N_2 and NH_3

* Corresponding author. Tel.: +7 095 9394079.
** Corresponding author.
E-mail addresses: peskov@cs.msu.su (N.V. Peskov), slinko@polymer.chph.ras.ru (M.M. Slinko).

0920-5861/$ – see front matter © 2005 Elsevier B.V. All rights reserved.
doi:10.1016/j.cattod.2005.02.044

production rates. The results of simulations for Rh(1 1 1), Rh(5 3 3) and Ir(1 1 0) showed that for these single crystal planes the key elements of the oscillatory mechanism responsible for the phase shift between N_2 and NH_3 production rates are periodic transitions between N- and O-rich surfaces due to the lateral interactions in the adsorbed layer. In this case, the phase shift between the N_2 and NH_3 production rates are due to repulsive interactions between N_{ads} and O_{ads}, poisoning of the surface for dissociative adsorption of hydrogen by N_{ads} and accumulation of O_{ads} that blocks NO dissociation.

Recently, oscillatory behaviour was discovered for the $N_2O + H_2$ reaction over the Ir(1 1 0) single crystal surface [8]. The reaction products are N_2 and H_2O. N_2O oscillates in counter-phase with N_2 and the maximum in H_2O formation is ''delayed'' compared to the maximum in N_2 formation [8]. A change of the reducing component from hydrogen to CO reveals even more interesting and puzzling properties of oscillations. It was discovered that not only the products N_2 and CO_2 oscillate nearly in counter-phase, but also the reactants N_2O and CO produce counter-phase oscillations [9]. To our knowledge, this is the first observation of a phase shift between the two reactants participating in one oscillating reaction. Earlier, counter-phase oscillations between the reactants CH_4 and NO have been detected for the oxidation of a mixture of $CH_4 + NO$ over titania-supported Pd catalysts [10]. However, in this case two reactions of methane oxidation, namely $CH_4 + O_2$ and $CH_4 + NO$ proceed simultaneously and oscillatory behaviour originates due to periodic oxidation and reduction of Pd. Counter-phase oscillations originate, because NO reduction to N_2 by CH_4 is the dominant reaction on the reduced phase, whereas on the oxidized phase the direct oxidation of methane prevails.

The goals of the present study are: (1) the analysis of the possible causes of oscillations during the $N_2O + H_2$ and $N_2O + CO$ reactions over the Ir(1 1 0) surface, (2) the development of mathematical models that can describe the experimentally observed oscillatory behaviour in these systems and (3) to explain the origin of the phase shifts between the oscillations in reactant concentrations, as well as the phase shifts between the oscillations in reaction products.

2. Experimental observations

Reactions were performed in a UHV system (Leybold Heraeus) equipped with facilities for LEED, AES and a differentially pumped (60 L/s) quadrupole mass spectrometer (UTI 100 C). The system was pumped by a turbo molecular pump (170 L/s) and an ion pump (150 L/s). The base pressure was always better than 2×10^{-10} mbar. The crystal was cleaned by repetitive cycles of heating in an oxygen or hydrogen atmosphere, Ar^+ ion sputtering ($p(Ar) = 1 \times 10^{-5}$ mbar, incident energy = 1.5 kV) and flashing in UHV to 1400 K. The Ar^+ ion sputtering and flashing treatments were repeated at the beginning of each series of experiments and the surface cleanliness was checked by AES and LEED.

TDS measurements were performed by heating a sample with an adsorbed layer with a constant heating rate of 25 K/s. The desorbing species were monitored by a differentially pumped quadrupole mass spectrometer (QMS).

During the reactions, the crystal was turned in front of a small opening, which gave access to the QMS chamber. Reactions were performed in the flow mode using a turbomolecular pump.

High purity gases (Messer Griesheim, purity: 99.5–99.999%) were used without further purification. The pressure readings of the ion gauge were corrected using relative sensitivities for N_2O, H_2 and CO to N_2 of 1.0, 0.46 and 1.05, respectively. Since some species have the same mass (CO and N_2—mass 28, N_2O and CO_2—mass 44), the use of labelled CO (^{13}CO from Sigma–Aldrich) was required to distinguish them. To make reading easier it will be further referred in the text simply as CO. Further details of experimental procedures have been described elsewhere [8,9].

2.1. TDS experiments

The TDS studies revealed interesting features of N_2O decomposition on the Ir(1 1 0) single crystal surface. Fig. 1a shows TDS experiments carried out after N_2O exposure at 300 K. A single peak of mass 44 is observed around 425 K, slightly shifting to lower temperatures with increasing N_2O exposure. Fig. 1b shows two main peaks for mass 28 approximately at 435 (α) and 492 K (β) whose intensities decrease with increasing N_2O exposure. The presence of two desorption peaks for N_2 was also reported by other authors, however at much lower temperatures [11]. The first peak was attributed to decomposition of N_2O weakly bound to the clean surface and the second one to the decomposition of N_2O more tightly bound to the partially oxidised surface [11]. It should be noted that mass 28 is both a cracking fragment of N_2O and the parent peak of N_2. Hence, the 28 peaks at 435 K is for a small part due to N_2O desorption. The different variation of the 44 and 28 peaks with exposure shows that the 28 peaks are mainly due to N_2 formation. It was demonstrated that CO_2 and CO did not contribute to the spectra shown in Fig. 1 [8].

The presented results show that N_2O can dissociate on the Ir(1 1 0) surface to N_2 and O_{ads}. No mass 30 (NO) was detected in TDS spectra. Surprisingly, N_2O desorption has been observed at temperatures higher than 300 K. The intensities of the two desorption peaks for N_2 decreased with increasing N_2O exposure. Therefore, the influence of oxygen pre-coverage on the character of the TDS spectra has been studied.

Fig. 2a and b shows the TDS experiments after exposing the sample to 2.5 L N_2O at 300 K, on a surface pre-covered

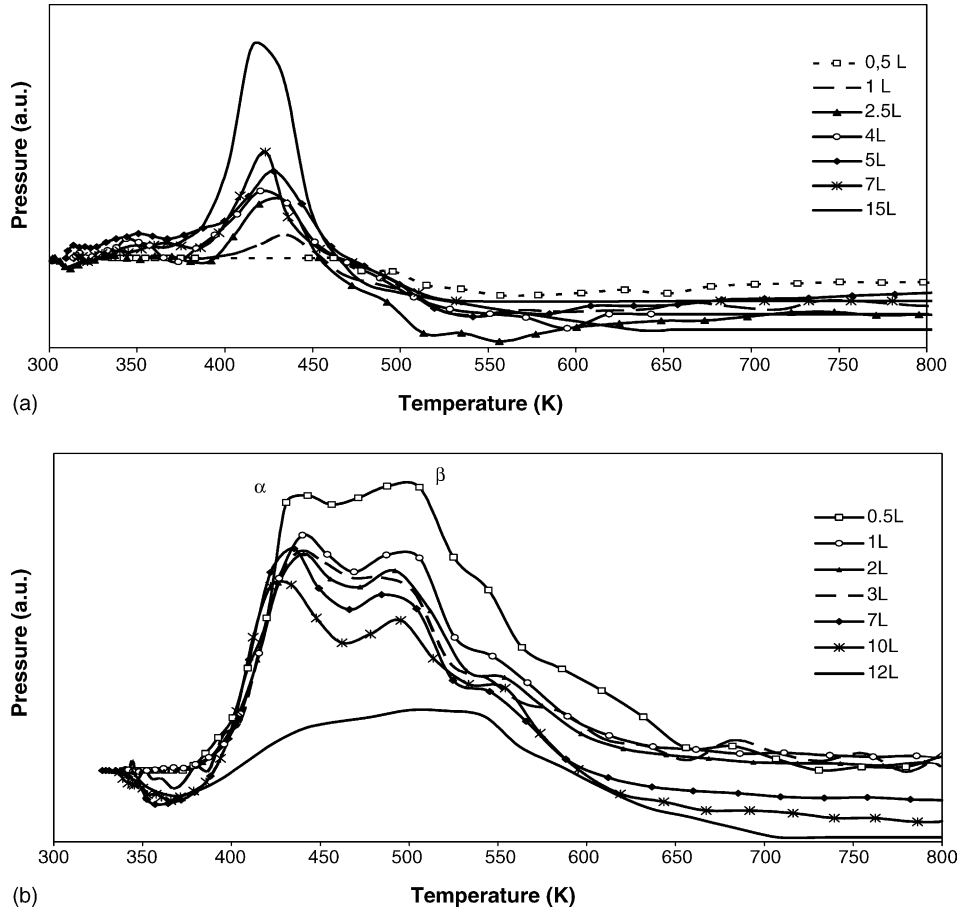

Fig. 1. TDS experiments carried out on the Ir(1 1 0) surface, after N_2O exposure at 300 K, for mass 44 (a) and mass 28 (b), at a heating rate of 25 K/s.

with oxygen. There is a large increase in the peak of mass 44 (Fig. 2a) with increasing O_2 pre-coverage. To what concerns mass 28 (Fig. 2b), the α peak originally present at lower temperatures, without oxygen pre-coverage, disappears when the surface is covered with oxygen. However, the β peak (also seen without oxygen pre-coverage) increases greatly following a previous exposure to 0.05 L O_2. At higher pre-coverage of oxygen, the β peak intensity decreases, disappearing following a 1 L pre-exposure of O_2.

These results show that the adsorbed oxygen does increase the rate of N_2O desorption in the temperature range around 450 K. Moreover, oxygen modifies the rate of N_2O decomposition in a very complicated manner. At small oxygen pre-coverages acceleration of N_2O decomposition takes place, whereas at higher oxygen coverages inhibition of this process is found.

2.2. Oscillatory behaviour during $N_2O + H_2$ and $N_2O + CO$ reactions over Ir(1 1 0)

Oscillatory behaviour has been observed at a N_2O pressure of 1×10^{-6} mbar in the temperature range between 460 and 464 K for the $N_2O + H_2$ reaction and between 373 and 377 K for the $N_2O + CO$ reaction. For both systems, oscillations were observed in a very narrow temperature region and values of reductant/N_2O ratio (R) shown in Table 1.

As can be seen from Table 1 oscillations during $N_2O + CO$ reaction can be observed at smaller values of R and lower temperatures than for the $N_2O + H_2$ reaction. For both systems at higher temperatures, oscillations are detected at smaller values of R. In both systems, oscillations were obtained by slowly heating the crystal in N_2O (1×10^{-6} mbar) with a very low amount of H_2 or CO (H_2/N_2O ratio of approximately 0.4 and CO/N_2O ratio close to 0.1) from room temperature to 800 K and subsequent cooling to the temperature of the oscillatory region. Then, the pressure of H_2 or CO was increased stepwise until sustained oscillations in rate started.

Fig. 3 shows oscillations in the partial pressures of N_2O, H_2O and N_2 detected at 460 K for a N_2O pressure of 1×10^{-6} mbar and a H_2/N_2O ratio of 1.2. As can be seen from Fig. 3 the variations of N_2O pressure are very small and the product N_2 pressure oscillates in counter-phase with the reactant N_2O pressure. However, it is also noted that the oscillations in H_2O formation are ‘‘delayed’’ compared to the oscillations in rate of N_2 formation. Fig. 4 shows the oscillatory behaviour of the $N_2O + CO$ reaction at 375 K for

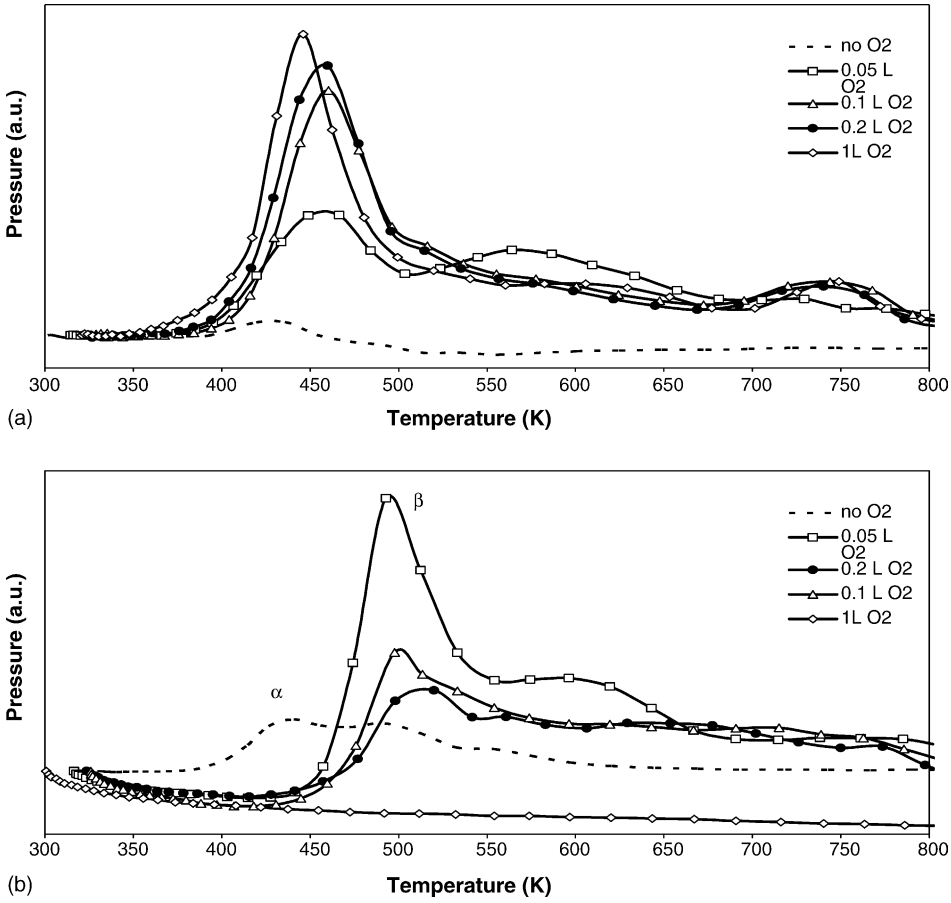

Fig. 2. TDS experiments carried out on the Ir(1 1 0) surface, after 2.5 L N_2O exposure at 300 K, on a surface pre-covered with oxygen, for mass 44 (a) and mass 28 (b), at a heating rate of 25 K/s.

a CO/N_2O ratio equal to 0.1. The product N_2 oscillates in counter-phase with the reactant N_2O and the CO_2 pressure oscillates in counter-phase with the pressure of the other reactant CO. The most striking result is that the pressure of the reactant N_2O oscillates in an almost counter-phase relationship with the oscillations of the other reactant CO. This results in nearly counter-phase oscillations of the N_2 and CO_2 production rates.

Figs. 3 and 4 show that the shape and the character of oscillations for various reactions are similar. In both systems, the period of oscillations is approximately 60 s in spite of different temperatures at which oscillations have been detected.

Table 1
Comparison of the conditions of the oscillatory region for $N_2O + H_2$ and $N_2O + CO$ reactions

Oscillations in $N_2O + H_2$ reaction		Oscillations in $N_2O + CO$ reaction	
$R = H_2/N_2O$	Temperature (K)	$R = CO/N_2O$	Temperature (K)
1.2	460	0.15	373
1.1	461	0.12	374
1	462	0.1	375
0.95	463	0.09	376
0.9	464	0.08	377

3. Discussion

There are some well-known feedback mechanisms, which can lead to the appearance of reaction rate oscillations under UHV conditions over single crystal surfaces. They are: surface phase transitions and periodic oxidation–reduction of the sub-surface catalyst layer [1,12]. In the present case, the surface phase transition as the origin of oscillations can be excluded. According to the literature data the reconstruction of the Ir(1 1 0) single crystal surface is lifted only by oxygen adsorption and only at temperatures higher than 700 K [13]. In comparison with the Pt(1 1 0) and Pd(1 1 0) surfaces, sub-surface oxygen on the Ir(1 1 0) surface is much more tightly bound and rather unreactive. Moreover, the initial sticking coefficient for oxygen is even higher on the surface oxide of Ir(1 1 0) than on the clean surface [13]. This explains, why no oscillations due to a periodic oxidation–reduction of the sub-surface layer similar to the Pd(1 1 0) single crystal surface have been detected during CO oxidation over Ir(1 1 0) [14].

Recently, it was demonstrated for NO reduction that lateral interactions in the adsorbed layer might be the origin of oscillatory behaviour [15,16]. In the system under investigation, the complicated variation of the TD spectra

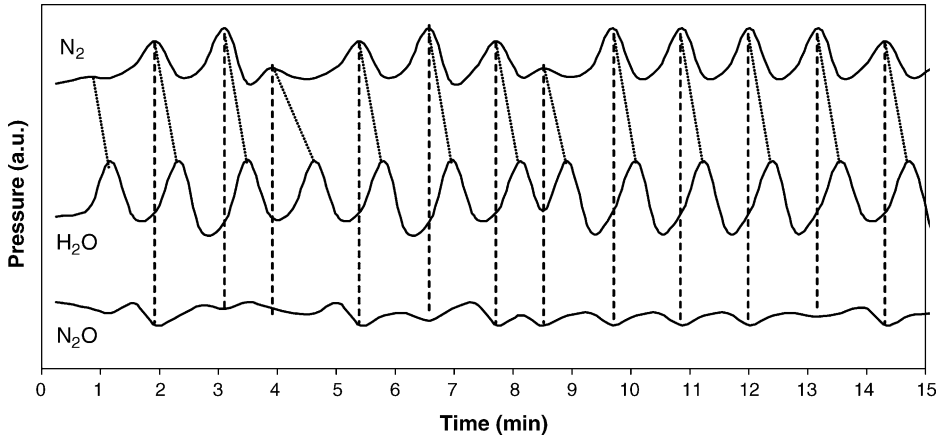

Fig. 3. Oscillations in the partial pressures of N_2O, H_2O and N_2, on the Ir(1 1 0) surface, at a N_2O pressure of 1×10^{-6} mbar. The temperature was 460 K and the H_2/N_2O ratio was 1.2.

with the change of the amount of pre-adsorbed oxygen points to the presence of lateral interactions. To understand the character of the lateral interactions, which cause the oscillatory behaviour of the N_2O reduction reactions over Ir(1 1 0) surface mathematical modeling was used.

Analysis of the properties of oscillations demonstrates that the oscillatory behaviour observed is very similar for the $N_2O + H_2$ and $N_2O + CO$ reactions. In both cases, the temperature of the appearance of oscillations decreases with an increase of the reductant/N_2O ratio (R). The shape and period of oscillations in both systems are also very similar. These data might indicate that the main origin of the oscillatory behaviour is the same in both cases.

3.1. Mathematical model of rate oscillations for the $N_2O + H_2$ reaction

The reaction mechanism of the $N_2O + H_2$ reaction includes adsorption/desorption of N_2O, and the dissociation steps of H_2 and N_2O. According to TDS studies [8], the reaction products N_2 and H_2O, produced at $T > 400$ K, desorb immediately after their formation on the catalyst surface.

$$\begin{aligned}
&N_2O_{(g)} + [M] \underset{k_{-1}}{\overset{k_1}{\Leftrightarrow}} [M - N_2O],\\
&H_{2(g)} + 2[M] \underset{k_2}{\overset{k_{-2}}{\Leftrightarrow}} 2[M - H],\\
&[M - N_2O] \overset{k_3}{\Rightarrow} N_{2(g)} + [M - O],\\
&[M - O] + 2[M - H] \overset{k_4}{\Rightarrow} H_2O_{(g)} + 3[M].
\end{aligned} \tag{1}$$

Mathematical modeling has been done on a macroscopic level and is based on the standard mean field approximation. To develop the mathematical model in its simplest form the following assumptions are made:

(1) H_2 and N_2O adsorption proceed on separate sub-lattices of surface adsorption centres;
(2) the variations of the gas phase partial pressures p_{N_2O} and p_{H_2} are very small during the reaction.

Following the proposed reaction mechanism, one arrives at a set of three coupled ordinary differential equations

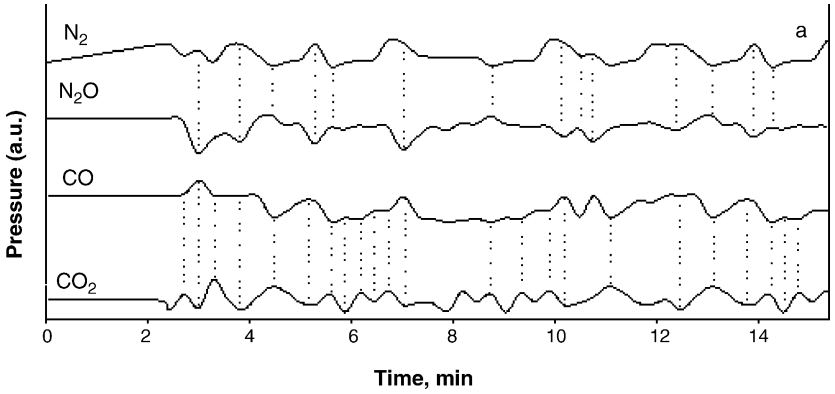

Fig. 4. Oscillations in the partial pressures of N_2O, N_2, CO and CO_2, on the Ir(1 1 0) surface at a N_2O pressure of 1×10^{-6} mbar and 375 K. CO/N_2O ratio was 0.1.

(ODE), describing the temporal variation of average surface coverages of N_2O (x), O (y) and H (z):

$$\begin{aligned} x' &= k_1 p_{N_2O}(1-x-y) - k_{-1}x - k_3 x, \\ y' &= k_3 x - k_4 y z^2, \\ z' &= k_2 p_{H_2}(1-z)^2 - k_{-2} z^2 - k_4 y z^2; \end{aligned} \tag{2}$$

where p_{N_2O} and p_{H_2} are the partial pressures of N_2O and H_2.

At any positive values of the rate constants k_i, where $i = \pm 1, \pm 2, 3, 4$, and $k_2 p_{H_2} \neq k_{-2}$, the system (2) has two stationary solutions. One of these solutions belongs to physical domain $x \geq 0$, $y \geq 0$, $x + y \leq 1$ and $0 \leq z \leq 1$. At reasonable values of k_i, the physical stationary solution is stable whereas the unphysical one is unstable and numerical analysis of the system (2) does not reveal any limit cycle solutions. To obtain oscillations the lateral interactions in the adsorbed layer were introduced in the model. The non-ideality of the adsorbed layer was accounted for through the dimensionless parameters of lateral interactions $e_{i,x}$, $e_{i,y}$ and $e_{i,z}$, where i denotes the number of the step. The rate constants k_i are supposed to be expressed in the following form:

$$k_i = k_i^0 \exp\left[-\frac{E_i}{RT}\right] \times \exp\left[\frac{T_0}{T}\left(e_{i,x}x + e_{i,y}y + e_{i,z}z\right)\right], \tag{3}$$

with $T_0 = 460$ K. On the basis of the TD spectra shown in Figs. 1 and 2 it was supposed that due to lateral interactions adsorbed oxygen accelerates the rate of N_2O desorption and the rate of N_2O dissociation, i.e. $e_{-1,y}, e_{3,y} > 0$. The bifurcation analysis based on the path-following technique demonstrated that the critical parameter for oscillations is $e_{3,y}$. Fig. 5 shows the dependence of the stationary solution of the system (2) belonging to the physical domain versus the parameter $e_{3,y}$. Black circles depict locations of the Andronov–Hopf bifurcations points h_1 at $e_{3,y} = 9.935$, and h_2 at $e_{3,y} = 10.958$. Between the points h_1 and h_2 the stable limit cycle solution of the system (2) exists. The path-following technique also demonstrated that parameter $e_{-1,y}$ practically does not affect the location and the length of the $e_{3,y}$ oscillatory interval at least for $-5 < e_{-1,y} < 5$.

The values of reaction stages constants are given in Table 2. The impingement rates of the gases given by the constants k_1 and k_2 have been calculated for $T = T_0 = 460$ K with kinetic gas theory using literature data for the initial sticking coefficients s_0. The literature data give $s_0 = 0.97$ for hydrogen adsorption and $s_0 = 0.95$ for oxygen adsorption.

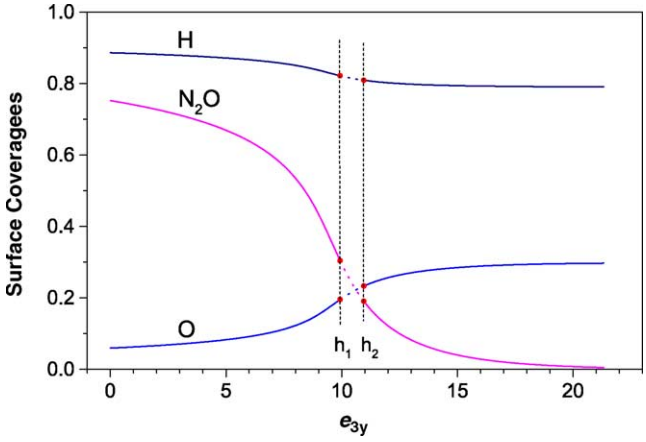

Fig. 5. Bifurcation diagram of the physical stationary solution of system (2) in dependence on the parameter $e_{3,y}$ at rate constants values given in Table 2. Solid lines—stable solution and dotted lines—unstable solutions.

No data is available in the literature concerning the parameters for N_2O desorption and dissociation rates. The frequency factors and values of activation energies of these steps are estimated by fitting the experimental data. As unknown parameters remain the ones of lateral interactions $e_{-1,y}$ and $e_{3,y}$. They are also estimated by fitting the boundaries of the oscillatory region, obtained in the experimental study. The values of these parameters were found to be $e_{-1,y} = 4$ and $e_{3,y} = 10$.

The results of the bifurcation analysis at the chosen values of parameters are presented in Fig. 6. They show the phase diagram of the system (2) in the plane (p_{H_2}, T). The solid line denotes the line of the Andronov–Hopf bifurcation and the dashed line represents the line of a saddle-node bifurcation. The grey area shows the region of oscillations. As can be seen from this figure, the temperature region where oscillatory solutions originate is rather narrow. This fact is in excellent agreement with the experimental observations.

Fig. 7 displays oscillatory behaviour of the coverage of the adsorbed species, obtained as a result of mathematical modeling. The period of oscillations and the conditions of their appearance closely coincide with the experimental data. Fig. 8 shows oscillations in the production rate of H_2O and in the rate of N_2O decomposition. The last value coincides with the rate of N_2 formation, because following experimental data N_2 molecules desorb immediately after their formation on the catalyst surface.

Table 2
Pre-exponential factors and activation energies of various steps of the reaction mechanism (1) used in the simulations

k	k_1	k_{-1}	k_2	k_{-2}	k_3	k_4
k_0[a]	6.2×10^4	10^{13}	5.0×10^{22}	2.58×10^8	9.69×10^{22}	3.04×10^6
E [kal/mol]	0	35000	12348	23000	52250	15000
k[b]	0.062	0.001	0.014	0.003	0.014	0.225

[a] Dimension of k_1 and k_2 is $(\text{s mbar})^{-1}$, dimension of k_i for $i = -1$, -2, 3 and 4 is s^{-1}.
[b] The value of the constant at $p_{N_2O} = 10^{-6}$ mbar, $p_{H_2} = 1.2 \times 10^{-6}$ mbar and $T = 460$ K.

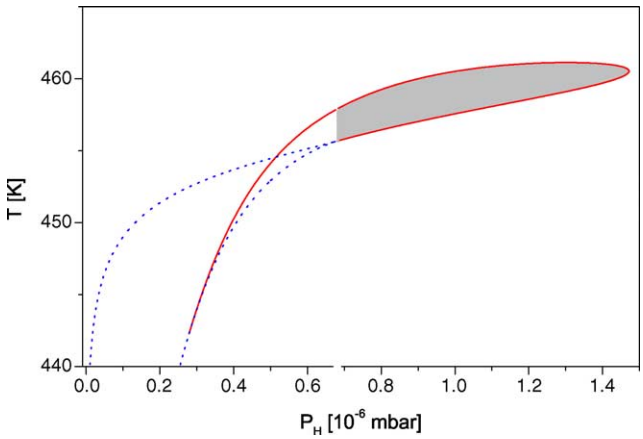

Fig. 6. The phase diagram of model (2) at $p_{N_2O} = 10^{-6}$ mbar. The grey area shows the region of oscillations.

As in the experiment the oscillations in H_2O formation are ''delayed'' compared to the oscillations in rate of N_2 formation. The mechanism of oscillations may be presented as follows: starting with the clean surface, hydrogen immediately occupies all sites on its sub-lattice and the concentration of N_2O on the other type of surface increases. Due to the dissociation of N_2O the concentration of adsorbed oxygen increases. Oxygen accelerates N_2O dissociation and the N_2O surface concentration drastically decreases while the O coverage increases in an autocatalytic way. However, due to the reaction with hydrogen the concentration of surface oxygen starts to decrease. The decrease of the oxygen concentration causes an increase of the N_2O surface concentration. As a result of this process the rate of N_2O dissociation again increases, leading to an increase of the surface concentration of oxygen. Oxygen again begins to accelerate the N_2O dissociation rate and the cycle of oscillations starts again.

Following this mechanism hydrogen has a minor role in the appearance of oscillations. Its task is only to modify the surface oxygen concentration and, hence, it affects the rate of N_2O dissociation. Therefore, the same mechanism may

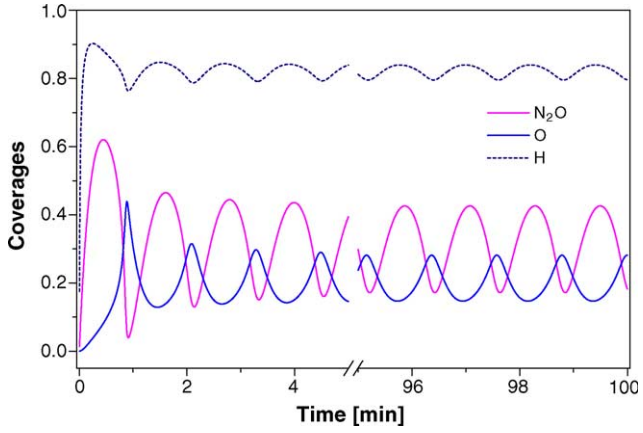

Fig. 7. Oscillatory behaviour of surface coverages at $p_{N_2O} = 10^{-6}$ mbar, $p_{H_2} = 1.2 \times 10^{-6}$ mbar and $T = 460$ K.

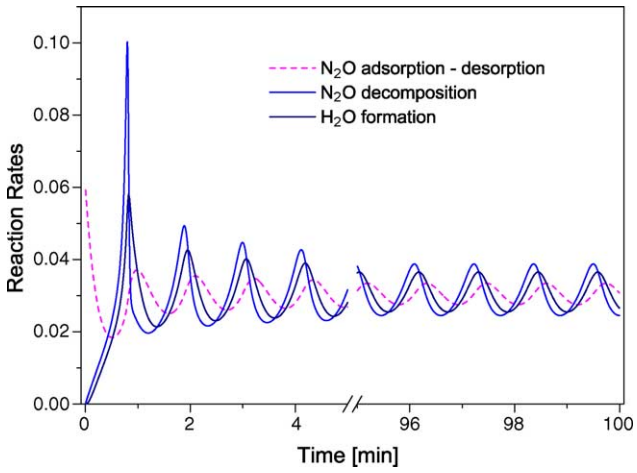

Fig. 8. Rates of N_2O decomposition and H_2O formation at the same conditions as in Fig. 7.

be valid for the oscillatory behaviour of the $N_2O + CO$ reaction.

3.2. Mathematical model of rate oscillations for the $N_2O + CO$ reaction

The mechanism of the $N_2O + CO$ reaction may be formulated in a way similar to the mechanism (1) for the $N_2O + H_2$ reaction. It contains adsorption, desorption of N_2O, CO and the N_2O dissociation steps:

$$\begin{aligned} &N_2O_{(g)} + [M] \overset{k_1}{\underset{k_{-1}}{\Leftrightarrow}} [M - N_2O], \\ &CO_{(g)} + [M] \overset{k_2}{\underset{k_{-2}}{\Leftrightarrow}} [M - CO], \\ &[M - N_2O] \overset{k_3}{\Rightarrow} N_{2(g)} + [M - O], \\ &[M - O] + [M - CO] \overset{k_4}{\Rightarrow} CO_{2(g)} + 2[M]. \end{aligned} \tag{4}$$

However, there is an essential difference between the $N_2O + CO$ and $N_2O + H_2$ reactions over Ir(1 1 0). Whereas there is no inhibition effect of the $N_2O + H_2$ reaction by hydrogen, CO inhibits the $N_2O + CO$ reaction when present in higher concentrations [9]. The inhibitory effect originates due to the competition for free adsorption sites and the competitive adsorption was introduced in the mathematical model.

The dynamic behaviour of the surface coverage can be described by the following system of differential equations, corresponding to mechanism (4):

$$\begin{aligned} x' &= k_1 p_{N_2O}(1 - x - y - z) - k_{-1}x - k_3 x, \\ y' &= k_3 x - k_4 yz, \\ z' &= k_2 p_{CO}(1 - x - y - z) - k_{-2}z - k_4 yz, \end{aligned} \tag{5}$$

where x denotes the N_2O coverage, y the O coverage and z is the CO coverage.

The amplitude of oscillations of the N_2O partial pressure was larger for the $N_2O + CO$ reaction than for the $N_2O + H_2$

reaction in spite of the lower temperatures at which oscillations were detected. Therefore, equation (5) was completed with equation (6), describing the dynamic behaviour of N_2O and CO partial pressures.

$$\begin{aligned} p'_{N_2O} &= \left(\frac{F}{V}\right)(P_{N_2O} - p_{N_2O}) \\ &\quad - \sigma(p_{N_2O}k_1(1-x-y-z) - k_{-1}x), \\ p'_{CO} &= \left(\frac{F}{V}\right)(P_{CO} - p_{CO}) \\ &\quad - \sigma(p_{CO}k_2(1-x-y-z) - k_{-2}z); \end{aligned} \tag{6}$$

with P_{N_2O}, P_{CO}—N_2O and CO inlet partial pressures, p_{N_2O}, p_{CO}—N_2O and CO pressures in the reactor, V—the reactor volume, F—the pumping rate. $\sigma = (SN_sRT)/V$, where N_s and S stands for the adsorption capacity and the catalyst surface area, respectively.

The variations of the N_2 and CO_2 partial pressures were simulated by the following differential equations:

$$\begin{aligned} p'_{N_2} &= -\left(\frac{F}{V}\right)p_{N_2} + \sigma k_3 x, \\ p'_{CO_2} &= -\left(\frac{F}{V}\right)p_{CO_2} + \sigma k_4 yz, \end{aligned} \tag{7}$$

where p_{N_2} and p_{CO_2} are the partial pressures of the products N_2 and CO_2, respectively.

Table 3 shows the values of parameters, which are known from the experimental data and were used in the simulations. The pre-factors and activation energies of the stages of the reaction mechanism (4) used in the simulations are given in Table 4. The impingement rate of CO given by the constant k_2 has been calculated for $T = T_0 = 375$ K with the kinetic gas theory using literature data for the initial sticking coefficient $s_0 = 1$ [17]. The values of pre-factors and activation energies of CO desorption and CO surface oxidation are in agreement with reactive thermal measurements of Taylor et al. [17].

Similar to the model (2) the system (5) has two stationary solutions: first solution is $X_1 = \{0, 1, 0\}$ and second solution can be expressed in the form $X_2 = \{x_2, y_2, z_2\}$, $y_2 = y_2(\mathbf{k})$, $x_2 = a(\mathbf{k})(1-y_2)$ and $z_2 = b(\mathbf{k})x_2$, where $\mathbf{k}$ is vector of rate constants k_i, $i = \pm1, \pm2, 3$ and 4. The solution X_2 is stable if it belongs to the physical domain $0 \le x,y,z \le 1$, $x + y + z \le 1$, and unstable otherwise. Under variation of parameters k_i the solution X_2 leaves (or enters) the physical domain at the point $X_2 = X_1$ with stability exchange between X_1 and X_2. Numerical analysis of system (5) did not reveal any limit cycle solutions at reasonable values of the constants k_i. Therefore, to simulate reaction rate oscillations lateral interactions must be considered. As in the previous case, here the lateral interactions are incorporated into the model via equation (3) with $T_0 = 375$ K.

Table 3
Parameters of the experimental study used in the calculations

F, pumping rate (cm^3/s)	42500
V, volume of the reactor (cm^3)	40000
S, Ir(1 1 0) surface area (cm^3)	0.56
N_s, the adsorption capacity (mol/cm^2)	1.67×10^{-9}

For the $N_2O + H_2$ system, the crucial feedback mechanism for the appearance of oscillations is the acceleration of N_2O decomposition by adsorbed oxygen. However, for $N_2O + CO$ this feedback mechanism turns out to be necessary but not a sufficient condition for the generation of the oscillatory behaviour. The essential difference between the models (2) and (5) is the difference in the adsorption of reducing agents. CO occupies the same adsorption centres as N_2O, while H_2 molecules adsorb on separate sub-lattice of adsorption centres. It was found that the rate oscillations in model (5) could arise if in addition to the acceleration of N_2O decomposition by adsorbed oxygen, CO adsorption is inhibited by adsorbed N_2O. Fig. 9 shows the bifurcation diagram of stationary solutions with respect to the variation of the parameter $e_{2,x}$ under fixed values of other parameters. When the parameter $e_{2,x}$ decreases from zero at the point $e_{2,x} \approx -0.320$ a saddle-node bifurcation takes place and in addition to the stationary solutions X_1 and X_2 a new pair of stationary solutions are emerged in the physical domain. One of the new solutions is stable and the other one is unstable. Soon with further decreasing of $e_{2,x}$ at point $e_{2,x} \approx -0.327$ the supercritical Andronov–Hopf bifurcation happens on the stable solution and stable limit cycle solution is established that vanishes at the second Andronov–Hopf bifurcation at $e_{2,x} \approx -3.158$.

From literature data it is known that for the $CO + O_2$ reaction CO can inhibit the CO_2 production rate [13]. Therefore, this type of lateral interactions was also included in the model. Another very important parameter for the simulation of the phase shift between the two reactants CO and N_2O is the parameter $e_{1,x}$. It was demonstrated that the value of the phase shift between p_{N_2O} and p_{CO} oscillations mainly depends on the value of this parameter. Fig. 10 demonstrates the projections of the phase trajectory of systems (5) and (6) in plane (p_{N_2O}, p_{CO}) for different values

Table 4
Pre-exponential factors and activation energies of the reaction mechanism (4) used in the simulations

k	k_1	k_{-1}	k_2	k_{-2}	k_3	k_4
k_0[a]	7.64×10^4	1.42×10^{11}	2.20×10^6	2.58×10^9	1.00×10^{18}	3.00×10^6
E [kal/mol]	0	25000	0	28000	36000	12000
k[b]	7.64×10^4	3.73×10^{-4}	2.20×10^6	1.21×10^{-7}	1.01×10^{-3}	3.01×10^{-1}

[a] Dimension of k_1 and k_2 is $(s\ mbar)^{-1}$, dimension of k_i for $i = -1$, -2, 3 and 4 is s^{-1}.
[b] The value of the constant at $P_{N_2O} = 10^{-6}$ mbar, $P_{CO} = 1.3 \times 10^{-7}$ and $T = 375$ K.

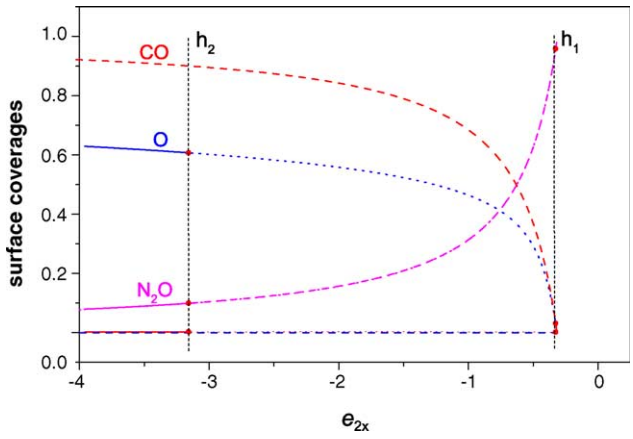

Fig. 9. Bifurcation diagram of the stationary state solutions of the system (5) in dependence of parameter $e_{2,x}$ at $e_{3,y} = 10$ and values of rate constants given in Table 4. Solid lines—stable solution and dotted lines—unstable solutions.

of $e_{1,x}$. The best description of the experimental data was obtained for $e_{1,x} = 6$. The final set of values of dimensional parameters of lateral interactions is presented in Table 5.

Fig. 11 shows the stationary solutions of systems (5) and (6) in dependence on T with the parameters from Tables 3–5. The bifurcation diagram shows that the stable limit cycle solution arises at T_h and exists at temperatures $T < T_h$ until it collides with the unstable solution X_1 (not shown) and disappears at $T \approx 300$ K. The rate of CO_2 production in the unsteady state together with the amplitude of the rate oscillations are shown in Fig. 12.

As can be seen from Fig. 12, the temperature region of oscillations in the model is larger than in the experimental study. However, the amplitude and period of oscillations depend greatly upon the temperature. At low temperatures the amplitude of oscillations diminishes and the period of oscillations increases. Fig. 13 demonstrates that at low

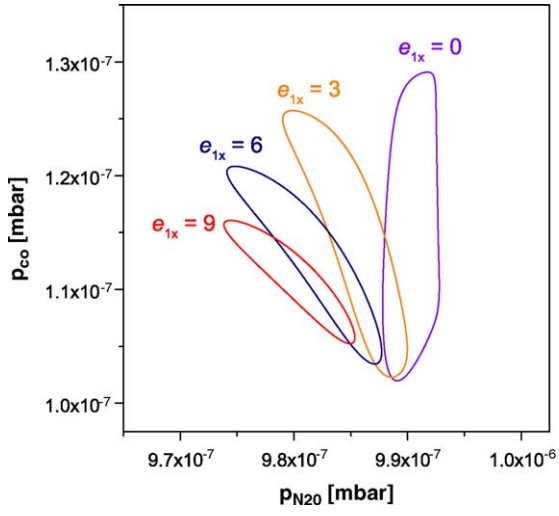

Fig. 10. The dependence of the phase shift between oscillations of p_{N_2O} and p_{CO} pressures upon parameter $e_{1,x}$.

Table 5
Dimensionless parameters of lateral interactions, which were used in the simulations

Stage 1	$e_{1,x} = 6$	N_2O activates N_2O adsorption
Stage 2	$e_{2,x} = -7$	N_2O inhibits the adsorption of CO
Stage 3	$e_{3,x} = 1.5$	N_2O activates N_2O decomposition
Stage 3	$e_{3,z} = 10$	O activates N_2O decomposition
Stage 4	$e_{4,y} = -3$	CO inhibits the CO + O reaction
Stage 4	$e_{4,z} = 1$	O activates the CO + O reaction

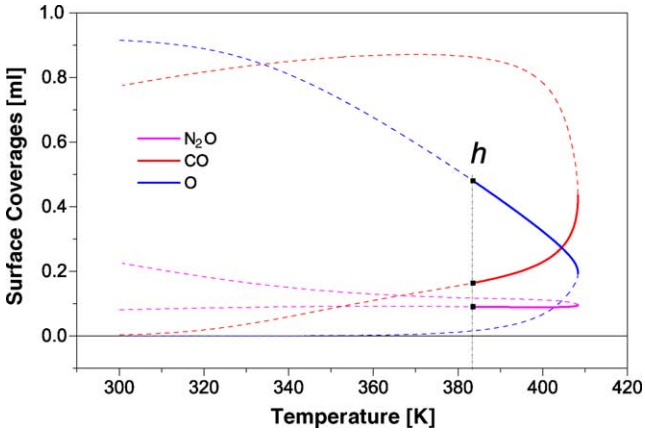

Fig. 11. The stationary solutions of models (5) and (6) vs. temperature T. Solid lines denote the stable solutions and dashed lines denote the unstable solutions. The black squares at $T_h = 384$ K mark the Andronov–Hopf bifurcation point.

temperatures the period of simulated oscillations may be as long as one hour. Small amplitude oscillations with such large period can be hardly detected in experimental studies.

The analysis of the dynamic behaviour of the system has been done with the help of equations (5)–(7). The oscillations of N_2O, CO, N_2 and CO_2 partial pressures are shown in Fig. 14. Similarly, to the experimental data the N_2O partial pressure oscillates in anti-phase with the N_2 partial pressure and the CO partial pressure oscillates in anti-phase

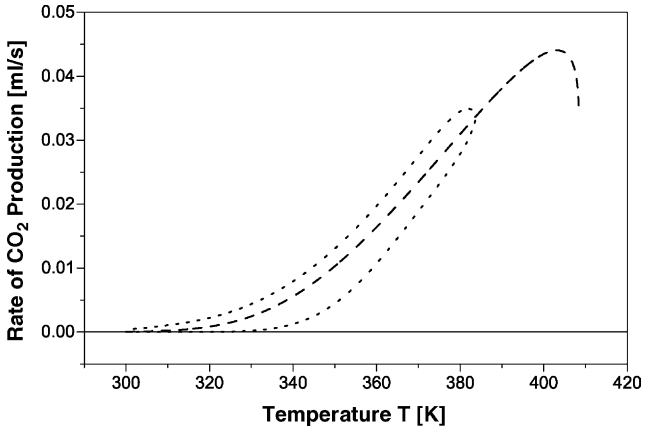

Fig. 12. The dashed line shows the rate of CO_2 production vs. the temperature. Dotted line indicates the amplitude of rate oscillations.

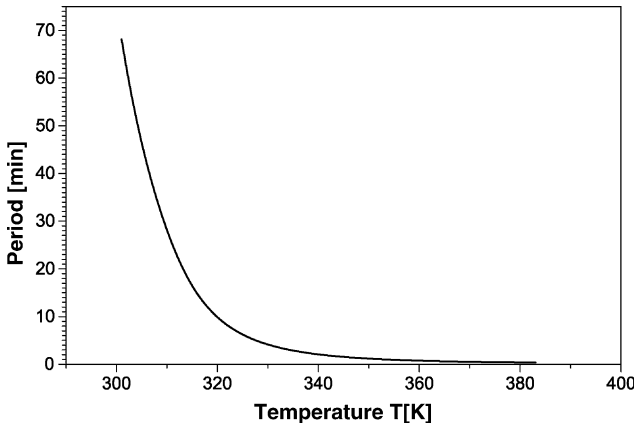

Fig. 13. The dependence of the period of limit cycle oscillations upon the temperature.

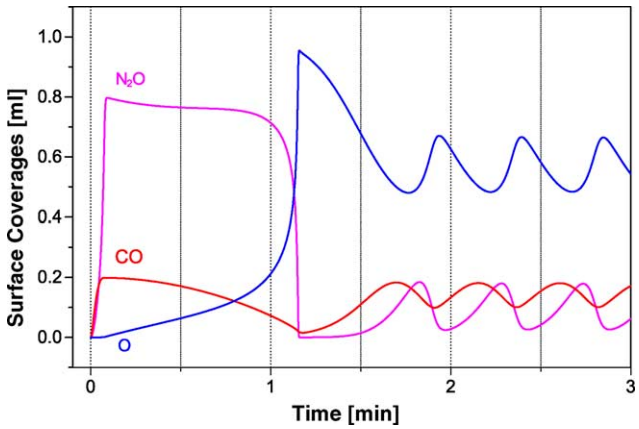

Fig. 15. Oscillatory behaviour of N_2O, CO and O surface coverages at 375 K.

with the CO_2 partial pressure. Moreover, the results of the simulation demonstrate that, as in the experimental results, the reactants N_2O and CO produce nearly anti-phase oscillations.

The mechanism of reaction rate oscillations during $N_2O + CO$ reaction is similar to the oscillatory mechanism in $N_2O + H_2$ system. The main feedback generating oscillations operates via the acceleration of N_2O decomposition by surface oxygen. However, the larger phase shift between oscillations of CO_2 and N_2 production rates in comparison with the $N_2O + H_2$ system originates due to the more complicated character of lateral interactions in the adsorbed layer. CO and N_2O adsorb on the same free sites and N_2O inhibits the process of CO adsorption.

Fig. 15 demonstrates the dynamic behaviour of surface coverages during $CO + N_2O$ reaction. It shows that the maximum of the rate of N_2 production coincides with the minimum of N_2O coverage and maximum of O coverage. Here, the rate of CO adsorption and CO coverage approach their maximum values. Due to the inhibition of the CO + O reaction rate by CO, the maximum in CO coverage coincides with the minimum in the CO_2 production rate. Therefore, both N_2 and CO_2 products will produce anti-phase oscillations. The phase shift between oscillations of N_2O and CO coverage is the result of anti-phase oscillations of N_2O and CO partial pressures. They originate due to the acceleration of N_2O decomposition by adsorbed oxygen, inhibition of CO adsorption by adsorbed N_2O molecules and inhibition of the CO + O reaction by adsorbed CO.

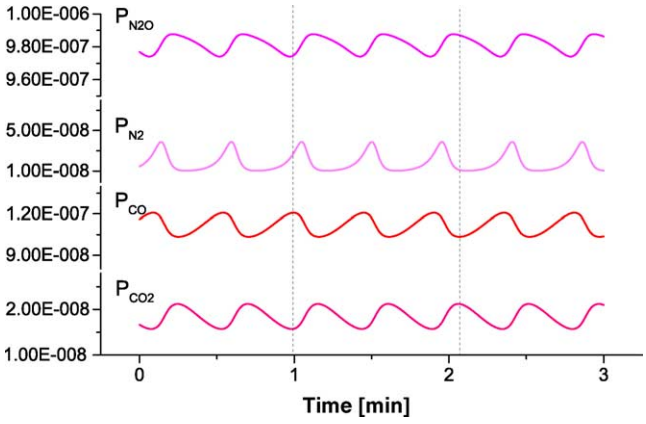

Fig. 14. Oscillations of N_2O, N_2, CO and CO_2 partial pressures at $T = 375$ K.

4. Conclusions

Two realistic mathematical models were developed which can reproduce almost quantitatively the region of existence and properties of the experimentally observed oscillatory behaviour of the $N_2O + H_2$ and $N_2O + CO$ reactions over the Ir(1 1 0) single crystal surface. It was shown that lateral interactions in the adlayer might be the origin of the observed oscillatory behaviour. In both systems the main feedback mechanism, generating oscillations operates via the acceleration of N_2O decomposition by oxygen. TDS studies demonstrated that such non-linear properties of the system could be detected only in a small region of N_2O and O coverages. This might be the explanation for the very narrow region of reactant partial pressures and temperature where oscillatory regimes were detected.

The main difference between oscillations in both systems is the value of the phase shift between oscillations of the partial pressures of the two products. Whereas the oscillation maximum for H_2O is only "delayed" compared to the maximum of N_2 oscillation, nearly anti-phase oscillations in the N_2 and CO_2 production rates were observed. The result of mathematical modeling shows that the larger phase shift of oscillations of CO_2 and N_2 production rates in comparison with the H_2O and N_2 production rates originate due to a more complicated character of lateral interactions in the adsorbed layer. In comparison to the $N_2O + H_2$ system, CO and N_2O adsorb on the same free sites and N_2O inhibits CO adsorption.

Acknowledgements

This work has been done in the framework of the programme for scientific cooperation between NWO and Russian Fund for Basic Researches (RFBR), Grant 047.015.002.

References

[1] M.M. Slinko, N.I. Jaeger, Oscillating Heterogeneous Catalytic Systems, Studies in Surface Science and Catalysis, vol. 86, Elsevier, Amsterdam, 1994.
[2] P. Hugo, M. Jakubith, Chem. Eng. Tech. 44 (1972) 383.
[3] V.D. Belyev, M.M. Slinko, V.I. Timoshenko, M.G. Slinko, Kinetika i Kataliz 14 (1973) 810.
[4] C.A. de Wolf, B.E. Nieuwenhuys, Catal. Today 70 (2001) 287.
[5] A.G. Makeev, B.E. Nieuwenhuys, J. Chem. Phys. 108 (1998) 3740.
[6] M. Gruyters, A.T. Pasteur, D.A. King, J. Chem. Soc., Faraday Trans. 92 (1996) 2941.
[7] S.J. Lombardo, T. Fink, R. Imbihl, J. Chem. Phys. 98 (1993) 5526.
[8] S.A. Carabineiro, B.E. Nieuwenhuys, Surf. Sci. 495 (2001) 1.
[9] S.A.C. Carabineiro, W.D. van Noort, B.E. Nieuwenhuys, Catal. Lett. 84 (2002) 135.
[10] U.S. Ozkan, M.W. Kumthekar, G. Karakas, J. Catal. 171 (1997) 67.
[11] Y. Matsumoto, J. Lee, H. Kato, K. Sawabe, SPIE-Proceedings 2125 (1994) 303.
[12] R. Imbihl, G. Ertl, Chem. Rev. 95 (1995) 697.
[13] J.L. Taylor, D.E. Ibbotson, W.H. Weinberg, Surf. Sci. 90 (1979) 37.
[14] S. Ladas, S. Kennou, N. Hartmann, R. Imbihl, Surf. Sci. 382 (1997) 49.
[15] A.G. Makeev, Math. Modell. 2 (1996) 115 (in Russian).
[16] A.G. Makeev, M.M. Slinko, N.M.H. Janssen, P.D. Cobden, B.E. Nieuwenhuys, J. Chem. Phys. 105 (1996) 7210.
[17] J.L. Taylor, D.E. Ibbotson, W.H. Weinberg, J. Chem. Phys. 69 (1978) 4298.